ACTIVATION RATE UNIFORMITY IN A BILATERAL IVNAA FACILITY FOR TWO ANTHROPOMORPHIC PHANTOMS

by

Hashem MIRI HAKIMABAD**, Lalle RAFAT MOTAVALLI, and Keihandokht KARIMI SHAHRI

Physics Department, School of Sciences, Ferdowsi University of Mashhad, Iran

Scientific paper
UDC: 544.431.12/.15:615.849.5
DOI: 10.2298/NTRP1002069M

Activation rate uniformity is the first property which is considered in the design of a prompt γ-ray *in vivo* neutron activation analysis facility. Preliminary studies on the activation rate distribution in the body can be done by use of Monte Carlo codes, such as the MCNP. In this paper, different bilateral configurations of an IVNAA system are considered in order to improve the activation rate uniformity in a water phantom measuring 32 cm 100 cm 16 cm. In the best case, uniformity parameters are $U = 1.003$ and $R = 1.67$, with the mean activation rate of 1.85 10^{-6} cm^{-3}. In more accurate calculations, the water phantom is replaced by a body model. The model in question is a 5 year-old ORNL phantom filled with just soft tissue. For uniformity studies, the internal organs are not simulated. Finally, uniformity parameters in this case are $U = 1.005$ and $R = 12.2$.

Key words: activation rate uniformity, prompt γ-ray IVNAA, bilateral configuration, MCNP code, phantom

INTRODUCTION

The prompt γ-ray *in vivo* neutron activation analysis (IVNAA) method has been employed for body composition measurements of humans and animals for the past forty years. At present, there are only seven IVNAA facilities around the world, built by individual research groups [1]. This non-destructive technique is a *gold standard* method for determining the total body nitrogen and one of the most precise ways to measure other essential body elements (such as hydrogen, carbon, calcium, *etc*.) [2-11]. So, the Neutron Activation Research Centre of Ferdowsi University of Mashhad has decided to develop a prompt γ-ray IVNAA facility. The three major points of prompt γ-ray IVNAA method that warrant the accuracy of measurements are: uniformity of activation rate distribution in the body, homogeneity in prompt γ-ray detection, and the low dose received by the patient. Therefore, in the first step, studies of activation rate uniformity in the body are in progress at present. Several researches were done on the smoothing of the activation function, particularly concerning depth [12-15]. However, less attention was paid to the uniformity of the activation rate distribution in the whole body. This paper and the previous one [16] are reports on design studies of an IVNAA system aimed at improving the activation rate uniformity. In this work, the ^{241}Am-Be is chosen as a neutron source in a bilateral configuration. In order to obtain the proper thicknesses of pre-moderators, moderators, and reflectors and determine the suitable collimator aperture, uniformity was investigated in depth, width, and length arrays of a water phantom (32 cm × 100 cm × 16 cm), in several setups. Also, collimator material was selected on the basis of uniformity parameters for the activation rate distribution in the entire body. Finally, instead of a water phantom, an anthropomorphic model was chosen. Uniformity parameters for the activation rate distribution in the entire body were estimated for a 5 year-old ORNL phantom [17, 18]. Calculations were performed using the MCNPX 2.4.0 Monte Carlo code [19].

* Corresponding author; e-mail: mirihakim@ferdowsi.um.ac.ir

MATERIALS AND METHODS

Facility description

The prototype of the prompt γ-ray IVNAA facility is assumed according to the recommendations of the previous work [16]. A water phantom measuring

32 cm × 100 cm × 16 cm is irradiated via a collimated neutron field produced by a bilateral configuration, up and down to the phantom. On each side, the collimator is an orthogonal parallelepiped void cast in a 40 cm × 40 cm 60 cm block which includes the collimator material. The ^{241}Am-Be neutron source is positioned at the centre of a 45 cm deep, 20 cm × 40 cm area graphite collimator. The 1.5 cm thick polyethylene pre-moderator is placed at 50 cm from the source (in the lower side, it is used as a bed). Two pairs of NaI(Tl) detectors are bilaterally positioned to the phantom.

To estimate the activation rate distribution, the phantom was latticed to about 3.200 cells of 4 cm × 4 cm 1 cm (LAT, U, and FILL cards).

To improve the uniformity of the activation rate in the exposed region of the sample, especially along its length and across the width, some of the system's parameters, such as the dimensions of the collimator aperture and collimator material, are changed. Moreover, moderators and reflectors are added to the phantom surfaces in order to reduce neutron losses and increase the thermal neutron flux near the surfaces. Figure 1 indicates the final version of the IVNAA facility designed in this paper.

Monte Carlo simulations

The MCNPX 2.4.0 code [19] was used to simulate the IVNAA setup and estimate the activation rate. MCNP codes are general purpose, continuous energy, generalized geometry, coupled neutron/photon/electron and time-dependent Monte Carlo transport codes. The cross-sections used in this project were chosen from the ENDF/B-VI libraries. Also, for neutrons below 4 eV, the $S(\alpha,\beta)$ scattering treatment was applied (MTm card). The neutron energy spectrum of a ^{241}Am-Be source was chosen from the IAEA report [20]. This paper focuses on activation rate distributions, thus the gamma rays from the source were ignored. The production rate of neutron-induced photons was assessed by use of a F4 neutron tally, along with the appropriate FM4 multiplier card.

Uniformity assessment

The uniformity of the activation rate in the region of interest should be as uniform as possible. To investigate the effects of the system's parameters on uniformity, activation rates are assessed in the cells of the latticed phantom for several configurations. The data were compared on the basis of the U index, defined as the ratio of the root mean square (rms) to the arithmetic mean of the estimated activation rate distribution

$$x_{\mathrm{rms}}^2 \quad \bar{x}^2 \quad \sigma_x^2$$

$$U \quad \frac{x_{\mathrm{rms}}}{\bar{x}} \quad \sqrt{1 \quad \frac{\sigma_x}{\bar{x}}^2}$$

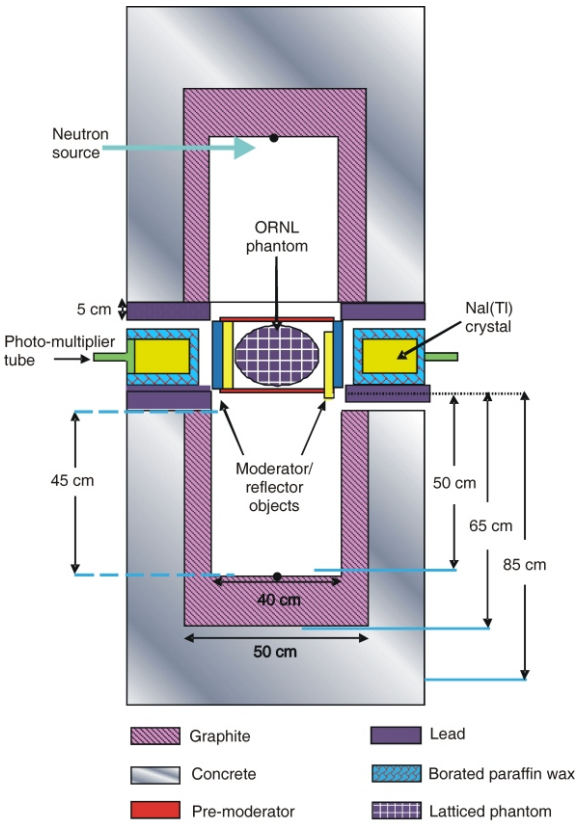

Figure 1. Schematic diagram of the final version of the IVNAA facility designed in the current study

where x_{rms}, $\bar{x}$ and σ_x are the rms, arithmetic mean, and the standard deviation of the distribution of the gamma production rate in the phantom, respectively. For more information, the maximum-to-minimum ratio of activation rate values is presented as R for all calculations.

ORNL phantom

In order to study the effects of sample size and shape on the activation rate distribution, the water phantom is replaced by a more accurate model of the body. Since the 5 year-old ORNL model [17, 18] is a good match in size (its height or length is about 110 cm, its width and depth are about 24 cm and 15 cm, respectively) with the water phantom, collimator aperture and other parts of the IVNAA facility, in this work, this phantom was selected as the sample.

This model was described in a series of ORNL mathematical phantoms by Cristy and Eckerman in 1987 [17] which follow the format of MIRD-type phantoms and represent adults and children of six age groups. A later, unpublished description, including modifications to the phantom models made subsequent to that publication (*e. g.*, refinements in the head and neck model) is presented in [18].

The phantom is composed of three major sections: (1) an elliptical cylinder representing the trunk

and arms which can be seen in fig. 1, (2) two truncated circular cones representing the legs and feet, and (3) an elliptical cylinder capped by a half ellipsoid representing the head, placed on top of a circular cylinder representing the neck. Attached to the leg section, there is a small region with a planar front surface containing the testes. Attached to the trunk, portions of two ellipsoids represent female breasts.

For uniformity studies, the internal organs were not simulated and the phantom was latticed to about 22.000 cells of 1 cm × 1 cm × 1 cm. The whole body is filled with soft tissue whose elemental composition and density were chosen from table A-1 of ORNL/TM8381 [17].

RESULTS AND DISCUSSION

Preliminary calculations show that depth distributions of the activation rate for all depth arrays (cells with the same width and length) in the latticed phantom exhibit the same behavior. In spite of some differences in the values of the gamma production rate, other parameters, such as U, show general similarities. The same goes for width and length distributions. Hence, studies on the effects of collimator aperture size, pre-moderators, moderators, and reflectors are done on the basis of the three given arrays: a depth array which lies at the centre of the sample and at the width and length arrays crossing points at the mid-depth of the phantom. This choice allows us to acquire a better understanding of the effects each of these variations in facility parameters have on the activation rate distribution. Besides, the required time for the MCNP program has been considerably reduced. Data uncertainties, in all cases, amount to less than 3%.

Depth distribution of the activation rate

Previously, the prompt gamma-ray IVNAA facility was improved in relation to the uniformity of the depth distribution of the activation rate [16]. Pre-moderators, positioned depth-wise next to the phantom surfaces, have the principal role of smoothing depth distribution in the given setup. The pre-moderator was a 15 mm-thick polyethylene which covered the upper and lower side of the exposed area of the phantom. Figure 2 compares the depth-functions of the gamma production rate on the basis of uniformity parameters, with and without the pre-moderator. Five pre-moderator thicknesses are considered: 5 mm, 8 mm, 10 mm, 15 mm, and 20 mm.

When the pre-moderator is absent, activation rate data in surfaces bellow 1cm of the phantom show great discrepancies with other points. The presence of polyethylene pre-moderators increases the thermal flux in the surface layers of the sample [13]. This thermal flux increment is caused by the slowing down of

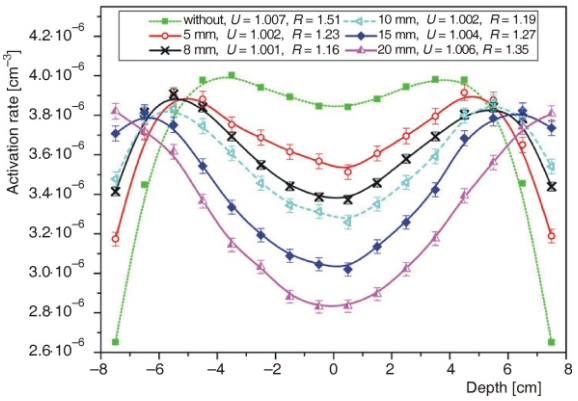

Figure 2. Activation rate distributions *vs*. the depth of the sample with their uniformity parameters for different pre-moderator thicknesses

some of the fast incident neutrons which penetrate the body in the absence of the pre-moderator. Such fast neutrons are thermalized and then captured in the deeper points of the phantom. Therefore, activation rate increment in the shallow regions is accompanied by its induction in the deeper zones. By increasing pre-moderator thickness, the thermal flux and gamma production rate near the surfaces are enhanced and the activation rate at the internal part decreased. At first, this process makes uniformity better, but only after given thickness distances between activation rates of deep and shallow points are increased. In the cases studied, the best thickness was 8 mm with good uniformity parameters: U = 1.001 and R = 1.16. From that point on, all simulations were done with a 8 mm thick polyethylene pre-moderator.

Collimator aperture

The effects of collimator aperture dimensions on the activation rate distribution have been investigated. As shown in fig. 3(a), for the 20 cm × 40 cm cross-sectional area, the uniformity of width distribution is not satisfactory, because gamma production decreases extremely at distances greater than 10 cm from the phantom centre, while the length distribution in the 18 cm area around the sample centre (36 cm in length) is uniform, with U = 1.002, see fig. 3(b), up to the region of 40 cm from the centre, with a linear slope of about 3.5% relative to the centre activation rate. At a distance of 40 cm to 50 cm from the sample centre, the slope decreases to about 1.3%. Judging by the results of length distribution, aperture size specifies the region where uniformity is achieved. Besides, beyond the aperture, activation declines at an admissible rate. If this is true, then the activation reduction near the lateral surfaces of the 30 cm thick phantom is justified. To examine the idea, a 30 cm width for the aperture was selected to cover the thickness of the phantom.

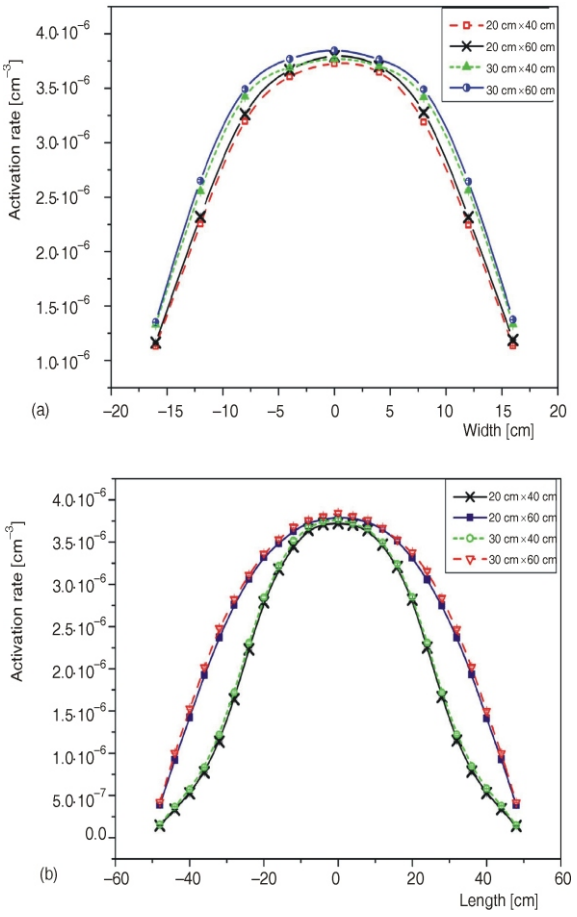

Figure 3. Activation rate distributions in four collimator aperture sizes versus (a) width and (b) length of the sample

Also, in order to extend the uniform part of the distribution length of the activation rate function, a length of 60 cm was tested. Accordingly, the collimator aperture was adjusted to dimensions of 20 cm × 40 cm, 20 cm × 60 cm, 30 cm × 40 cm, and 30 cm × 60 cm.

Table 1 lists *U* and *R* values for depth and width distributions of the activation rate. For length distributions, *U* values for the three intervals around the body centre are introduced as uniformity parameters. These intervals specify 22 cm, 26 cm, and 30 cm distances from the body centre that, respectively, represent 44 cm, 52 cm, and 60 cm long regions throughout the mid-depth of the phantom.

Table 1. Uniformity parameters of depth, width, and length distributions of the activation rate, for different collimator aperture sizes. *U* values of the length distributions are listed for three intervals around the body centre

Collimator aperture size [cm^2]		Uniformity parameters of activation rate distributions						
		Depth		Width		*U* values of the length		
		U	*R*	*U*	*R*	–22:22	–26:26	–30:30
20	40	1.001	1.14	1.072	3.30	1.005	1.014	1.030
20	60	1.001	1.16	1.070	3.26	1.001	1.003	1.006
30	40	1.001	1.16	1.057	2.83	1.005	1.013	1.028
30	60	1.001	1.16	1.056	2.85	1.001	1.002	1.005

As expected, *U* and *R* values of the depth distributions do not meaningfully change in the studied cases because these four situations differ only in transversal parameters. Table 1 shows that expanding the aperture cannot, in itself, significantly affect width distribution parameters, either: *U* values improve for about 1.3% and 1.4% in the case of 40 cm and 60 cm long apertures, respectively. Figure 3(a) clearly illustrates that width distribution functions for 30 cm wide apertures are not acceptable. The increment in aperture widths increases activation rates less than required. For example, the largest increment of about 15% occurred near the surface, while the value needed is around 70%. So, the uniformity of the width distribution of the activation rate should be dependent on other variables which are studied later.

As can be seen from fig. 3(b), lengthwise, activation rate distributions are constant when length parameters of the facility remain unchanged. Besides, the expansion of the aperture changes the shape of distribution functions. As a result, the uniform part extends to the distance of up to 26 cm from the sample centre, with $U = 1.003$ for 60 cm long apertures. Also, beyond the uniform region similar to the 40 cm long apertures, the linear slopes of curves are about 3.1% relative to the centre activation rate. Nevertheless, the activation rate of the uniform region is too great to be ignored. The 30 cm × 60 cm collimator aperture was selected for simulations presented next; however the desired uniformity has not been achieved, as of yet.

Transverse distribution of activation rate

Uniformity in the exposed region

Figure 3(a) shows that aperture size cannot significantly improve the reduction of activation rates near the lateral surfaces, unlike the smoother length distributions in the 60 cm-long collimator apertures. Upon further reflection, it seems that the intrinsic difference between width and length thicknesses of the phantom may be the cause of this dissimilarity. In other words, the presence of the sample material beyond the aperture, as a very good moderator, lengthwise, guarantees the thermal neutron flux in a relatively broad interval. While, when width is concerned, neutrons are lost at the surface of the subject. Therefore, in order to increase the thermal flux in this region and reduce neutron losses, moderator/reflector objects which cover the sides of the exposed area are introduced. The moderator should be sandwiched between the sample and the reflector, so as to slow down the fast neutrons scattered toward the sample by the reflector.

To find a suitable moderator/reflector object, water (H_2O) and polyethylene (CH_2) as moderator ma-

terials and graphite (C), as a reflector material, are examined in different compositions and thicknesses. Figure 4 illustrates some more smoothed width distributions. In first simulations, 30 cm × 60 cm dimensions are considered for the collimator aperture. But as can be seen from fig. 4, the activation rate near the surfaces does not increase as expected, even for the most uniform distribution. One way to solve this problem is to extend the collimator aperture width in order to enhance the neutron flux received by the moderator/reflector objects. So, new calculations were done for a collimator aperture of 40 cm × 60 cm. Table 2 summarizes *U* and *R* values of the activation rate distribution in connection to the width for eleven different moderator/reflector objects. The data is sorted on the basis of ascending values of uniformity.

Table 2 reveals that the employment of 40 cm wide collimator apertures makes the width activation rate distribution more uniform, with *U* values less than 1.002. It is, thus, clear from this table that in spite of the similarity between water and polyethylene data, water shows better values. This can, partly, be attributed to the greater density of water (1 g per cm^{-3} in comparison to 0.94 g per cm^{-3}). Besides, the most uniform cases have an 8 cm-thick moderator/reflector object. Therefore, a 5 cm-thick water and a 3 cm-thick graphite moderator/reflector object was selected for the next setups. The collimator aperture width was adjusted to 40 cm.

Activation in the unexposed region

In whole body scanning, uniformity is necessary in activation rate distribution at all points. It is desirable to design a facility so that the uniformity of the activation rate is achieved entirely in one phase. In such states, one measurement is enough. If it is not possible to attain uniformity in a single phase, measurements should be performed in several stages. The body is divided into several regions and in each step only one region of the phantom is irradiated. It is ideal that the activation rate distribution be smoothed for each phase and, also, that the activation in other regions is ignorable. The latter condition is necessary because, if the activation in the unexposed region is considerable, induced gamma rays in that region will be detected more than once. In other words, the total activation rate distribution, which is obtained from all measurements, will not be uniform. This is a problem that occurs in all length distributions of the activation rate.

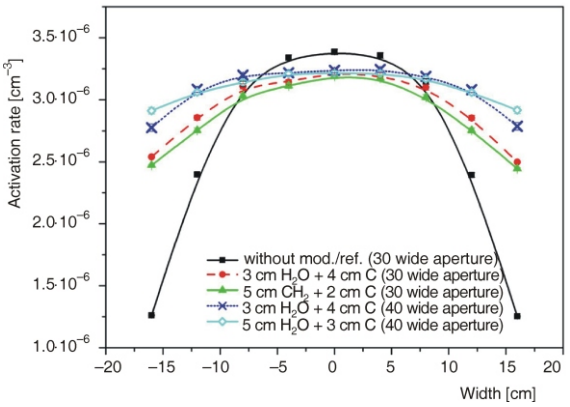

Figure 4. Comparison of width distributions of activation rates for different configurations with various lateral moderator/reflector objects and two values of collimator aperture width (30 cm and 40 cm)

Table 2. Uniformity parameters for several configurations of lateral moderator/reflector objects and two collimator aperture widths

Aperture width [cm]	Moderator		Graphite thickness [cm]	Uniformity	
	Material	Thickness [cm]		*U*	*R*
40	H_2O	5	3	1.001	1.10
40	H_2O	4	4	1.001	1.12
40	H_2O	3	5	1.001	1.13
40	CH_2	4	4	1.001	1.15
40	H_2O	3	4	1.002	1.17
40	CH_2	4	3	1.002	1.17
30	H_2O	3	4	1.004	1.29
30	CH_2	5	2	1.005	1.30
30	CH_2	3	4	1.005	1.31
30	CH_2	7	–	1.005	1.32
30	–	–	7	1.016	1.63

As shown in fig. 3(b), one cannot specify a given length interval wherein the activation rate distribution is uniform and its values are thus greater than the outer ones. This is true even for 40 cm-long collimator apertures. Extending the collimator aperture enlarges the uniform region lengthwise, but the activation rate beyond it also increases. Hence, the aim is to design the prompt gamma neutron activation analysis facility so that the entire uniformity of the activation rate is achieved in one phase. As can be observed, fig. 3(b), the reduction of the activation rate, especially beyond the collimator aperture area, destroys uniformity. Figure 5 shows that the 110 cm-long collimator aperture is not effective. Thermal neutron attenuation includes capture, scattering, and inverse square law effects, making the 75% reduction in the activation rate near the surfaces relative to its centre value. To reduce the thermal flux attenuation, in each up and down part of the facility, two similar neutron sources toward the length, four neutron sources totally, are utilized.

At each of the points of the phantom, activation rates from the two sources are superimposed and the minimum value occurs at the point most distant from both sources, *i. e*. in the middle. If the activation rate from each source decreases to 50% of its maximum at the middle point, it is expected that the activation rate distribution within the sources distance will become more smoothed. So, at first, for the distance between the two sources, for each of the sides, a distance of 80 cm was selected, based on the full width half maximum of the activation rate function of one neutron source. Each source is positioned at a distance of 40 cm from the collimator centre along the length and

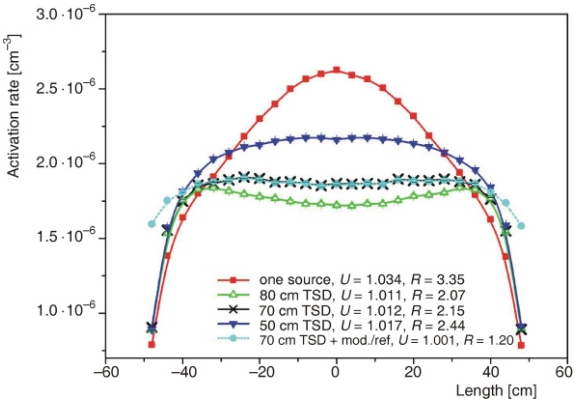

Figure 5. Length distribution of the activation rate obtained from one neutron source in each up and down part of the facility in comparison with the ones estimated for two neutron sources of various distances. Appending moderator/reflector objects to the front and back surface of the body is also being considered

at a 10 cm distance from the surface. But, especially at 20 cm from the body centre, the activation rate decreases (see fig. 5). Thus, the two sources become closer and calculations were repeated for both 70 cm and 50 cm sources distances. The reduction of the two sources distance (TSD) increases the activation rate in the middle of the phantom. The most smoothed function, within the 40 cm interval from the body centre, belongs to the facility with a 70 cm sources distance. Nevertheless, activation rate values near the body surfaces severely decreased in all cases. The same problem occurred in width distribution. In this study, two moderator/reflector objects with similar characteristics to those of the lateral ones are applied for length surfaces. Activation rate distribution is shown in fig. 5. As can be seen, appending the moderator/reflector objects does not change the middle of the activation function, while its values near the surfaces increase significantly. Uniformity parameters of these situations for the whole body length are listed in fig. 5. The results illustrate that the activation rate distribution becomes uniform (U = 1.001, R = 1.20) by the use of two sources in each collimator and a moderator/reflector object. The lengthwise design of the facility was adjusted based on the last studied case, namely a 70 cm TSD and a 5 cm thick water and 3 cm thick graphite moderator/reflector object.

Collimator material

Collimator material is the other factor investigated in this work. Polyethylene (CH_2), 5% boric-acid doped polyethylene (CH_2-B), and graphite (C) are the three materials upon which the uniformity of the activation rate is based. All suggestions from the previous sections were taken into account in the following calculations. In the new MCNP runs, activation rate values are estimated for all cells of the latticed phantom and uniformity parameters are calculated for all data. The results, summarized in tab. 3, indicate that the activation rate distribution in the body is acceptably uniform when the collimator material is graphite or borated polyethylene. Polyethylene cannot produce gamma rays uniformly, in comparison to the two latter materials. In comparison to borated polyethylene, graphite shows lower values of uniformity parameters. The other important advantage of graphite as a collimator material is its great activation rate. Graphite shows the biggest mean activation rate with a 100% and 60% growth relative to borated polyethylene and polyethylene, respectively. Therefore, graphite remains in force as a collimator material with good uniformity characteristics and a great activation rate to its advantage.

Table 3. *U* and *R* values of activation rate distributions in the whole body with their mean values for three collimator materials

Collimator material	Uniformity parameters		Mean activation rate [10^{-6} cm^{-3}]
	U	R	
C	1.003	1.67	1.43
CH_2-B	1.004	1.70	0.92
CH_2	1010	2.13	1.15

ORNL phantom

The design of the IVNAA facility is based on a simple water phantom. The differences in size and shape between the phantom and the real body definitely have a considerable effect on the activation rate distribution. It is, thus, clear that a more accurate model is necessary for the investigation of uniformity in the body. In this work, a 5 year-old ORNL model [17, 18] was chosen for the role of the anthropomorphic phantom. The parameters of the facility were adjusted as recommended in this paper. In the final calculation, the activation rate distribution is estimated throughout the latticed ORNL phantom for 22.000 cells, approximately. The said cells' volumes were chosen to be 16 times smaller than the previous ones, because some regions of the body, such as the neck, upper part of the head and lower parts of the legs are much less thick than some other parts of the body. It is expected that the variety of dimensions will reduce the thermal neutron flux and activation rate in the shallow cells of these slight parts because of the reduction in soft tissue which is a very good moderator. Such effects happened when width and length distributions in the water phantom were considered. So, the question remains: can moderator/reflector objects really improve uniformity?

To find the answer, whole body calculations by means of an ORNL phantom were done under three

different circumstances: (1) according to the final suggestions in the previous sections, (2) without the moderator/reflector objects, and (3) without moderator/reflector objects and pre-moderators. Table 4 lists the uniformity parameters for the three cases. Results show that uniformity parameters for the ORNL model, $U = 1.005$ and $R = 12.2$, increase in comparison to the water phantom. However, one cannot ignore the effect of moderator/reflector objects and pre-moderators on activation rate uniformity. Without moderator/reflector objects, the activation rate distribution is almost non-uniform and the removal of pre-moderators would only worsen the situation.

Table 4. *U* and *R* values of activation rate distributions in the ORNL phantom for three different situations

Moderator/reflector objects	Pre-mod	Uniformity parameters	
		U	*R*
Yes	Yes	1.005	12.2
No	Yes	1.034	19.6
Yes	No	1.044	24.4

For a more detailed study, fig. 6 displays a 3-D plot of activation rate values in a two dimensional array (32 width by 110 length) crossing at the mid-depth of the phantom. As expected, the absence of body tissue in the neck, upper part of the head and, especially, lower parts of the legs, reduces the thermal neutron flux and activation rate in these regions. In addition to this, the reduction of tissue thickness in lateral sides decreases the activation rate at the boundaries.

The use of a water phantom for improvement the uniformity led to the optimized IVNAA facility. The simple geometry of this model made following the optimization process easier, but there was concern that this simplicity was far from reality. Table 4 indicates optimized IVNAA facility increases uniformity of the activation rate distribution in the real body, although further studies are necessary in order to improve the uniformity to the more acceptable level.

CONCLUSIONS

This paper takes into consideration the design of a prompt γ-rays IVNAA facility aimed at improving the uniformity of the activation rate distribution in large biological samples. Activation rate values are calculated in the cells of a latticed phantom by using a MCNPX code. The effect of pre-moderator thickness is studied in relation to both depth distribution and 8 mm thick polyethylene, with $U = 1.001$ and $R = 1.16$ selected for the next setups. In order to smooth transverse distributions, width and length, two factors are tested: collimator aperture size and appending moderator/reflector objects to body surfaces. Width distribution can

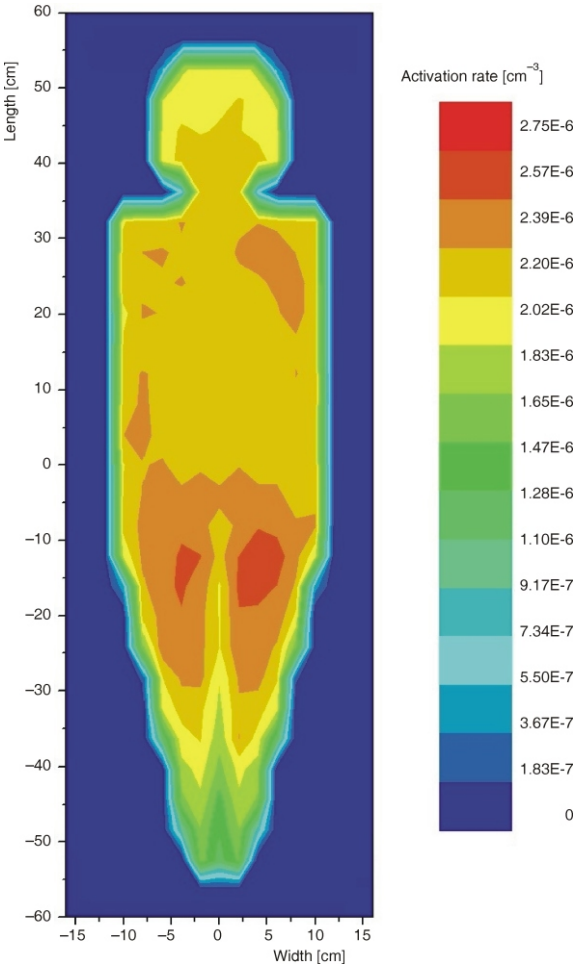

Figure 6. 3-D plot of activation rate values in a two dimensional array (32 width by 110 length) at mid-depth of the phantom

be uniform with a 5 cm-thick water and 3 cm-thick graphite moderator/reflector and a 40 cm-wide collimator aperture. Uniformity parameters are $U = = 1.001$ and $R = 1.10$. When length distribution is concerned, the one phase measurement is chosen to prevent the activation of the unexposed region of the body. Two neutron sources with a 70 cm distance in each of the up and down sides are employed and the length of the collimator aperture is adjusted to 110 cm. The moderator/reflector objects applied for length surfaces have similar characteristics to the lateral ones. The *U* and *R* values for length distribution become 1.001 and 1.20, respectively. Whole body calculations are done for three collimator materials. Graphite shows the smallest *U* and *R* values (1.003 and 1.67, respectively) and the greatest mean activation rate ($1.85\ \ 10^{-6}$ cm^{-3}). Therefore, graphite is confirmed for the next configuration studies. In more accurate calculations, the water phantom is replaced by 5 year-old ORNL model. Uniformity in the more real phantom is reduced to that of parameters $U = 1.005$ and $R = 12.2$. So, it can be concluded that there is a necessity for continuing studies on the uniformity of anthropomorphic phantoms.

REFERENCES

[1] Mitra, S., Body Composition to Climate Change Studies – the Many Facets of Neutron Induced Prompt Gamma-Ray Analysis, Nuclear and Radiochemistry Symposium (NUCAR 2009), BNL-81726-2008-CP, Brookhaven National Laboratory, January 7-10, Mumbai, India, 2009

[2] Mernagh, J. R., Harrison, J. E., McNeill, K. G., *In vivo* Determination of Nitrogen Using Pu-Be Sources, *Physics in Medicine and Biology, 22* (1977), 5, pp. 831-835

[3] Evans, H. J., Leblanc, A. D., Johnson, P. C., Facility for Regional *in vivo* Neutron Activation Analysis of Skeletal Calcium, *Physics in Medicine and Biology, 24* (1979), 1, pp. 181-187

[4] Ellis, K. J., Shypailo, R. J., Sheng, H. P., Pond, W. G., *In vivo* Measurements of Nitrogen, Hydrogen, and Carbon in Genetically Obese and Lean Pigs, *Journal of Radioanalytical Nuclear Chemistry, 160* (1992), 1, pp. 159-168

[5] Sutcliffe, J. F., A Review of *in vivo* Experimental Methods to Determine the Composition of the Human Body, *Physics in Medicine and Biology, 41* (1996), 5, pp. 791-833

[6] Ma, R., Ellis, K. J., Yasumura, S., Shypailo, R. J., Pierson, Jr. R. N., Total Body Calcium Measurements, Comparison of Two Delayed-Gamma Neutron Activation Facilities, *Physics in Medicine and Biology, 44* (1999), 6, pp. N113-N118

[7] O'Meara, J. M., Blackburn, B. W., Chichester, D. L., Gierga, D. P., Yanch, J. C., The Feasibility of Accelerator-Based *in vivo* Neutron Activation Analysis of Nitrogen, *Applied Radiation and Isotopes, 55* (2001), 6, pp. 767-774

[8] Chichester, D. L., Empey, E., Measurement of Nitrogen in the Body Using a Commercial PGNAA System – Phantom Experiments, *Applied Radiation and Isotopes, 60* (2004), 1, pp. 55-61

[9] Mattsson, S., Thomas, B. J., Development of Methods for Body Composition Studies, *Physics in Medicine and Biology, 51* (2006), 13, pp. R203-R228

[10] Kasviki, K., Stamatelatos, I. E., Kalef-Ezra, J., Evaluation of Spatial Sensitivity of a Prompt Gamma Neutron Activation Analysis Facility for the *in vivo* Determination of Nitrogen in Small Animals, *Journal of Radioanalytical Nuclear Chemistry, 271* (2007), 1, pp. 225-231

[11] Kasviki, K., Stamatelatos, I. E., Yannakopoulou, E., Papadopoulou, P., Kalef-Ezra, J., On the Accuracy of Protein Determination in Large Biological Samples by Prompt Gamma Neutron Activation Analysis, *Nuclear Instruments and Methods B, 263* (2007), 1, pp. 132-135

[12] Boddy, K., Elliot, A., Robertson, I., Mahaffy, M. E., Holloway, I., A High Sensitivity Dual-Detector Shadow-Shield Whole-Body Counter with an 'Invariant' Response for Total Body *in vivo* Neutron Activation Analysis, *Physics in Medicine and Biology, 20* (1975), 2, pp. 296-304

[13] Elliott, A., Holloway, I., Boddy, K., Haywood, J. K., Williams, D., Neutron Uniformity Studies Related to Clinical Total Body *in vivo* Neutron Activation Analysis, *Physics in Medicine and Biology, 23* (1978), 2, pp. 269-281

[14] Krishnan, S. S., McNeill, K. G., Mernagh, J. R., Bayley, A. J., Harrison, J. E., Improved Clinical Facility for *in vivo* Nitrogen Measurement, *Physics in Medicine and Biology, 35* (1990), 4, pp. 489-499

[15] Stamatelatos, I. E., Kasviki, K., Green, S., Gainey, M., Kalef-Ezra, J., Beddoe, A., Prompt-Gamma Neutron Activation Analysis Facility for *in vivo* Body Composition Studies in Small Animals, *Analytical and Bioanalytical Chemistry, 379* (2004), 2, pp. 192-197

[16] Hakimabad, M. H., Motavalli, R. L., Improvement the Uniformity of the Gamma Production Rate Distribution with Depth in a Large Biological Sample for an IVNAA Facility, *Nuclear Technology & Radiation Protection, 24* (2009), 2, pp. 119-125

[17] ***, Specific Absorbed Fractions of Energy at Various Ages from Internal Photon Sources, (Eds. M. Cristy, K. F. Eckerman), Oak Ridge National Laboratory Report ORNL/TM-8381/V1–7, Oak Ridge, Tenn., USA, 1987

[18] Eckerman, K. F., Cristy, M., Ryman, J. C., The ORNL Mathematical Phantom Series, Informal Paper, (Oak Ridge, TN: Oak Ridge National Laboratory), 1996, available at http://homer.hsr.ornl.gov/VLab/mird2.pdf

[19] ***, MCNPXTM User's Manual, Version 2.4.0. (Ed. L. Waters), Los Alamos National Laboratory Report LACP-02-408, Los Alamos, N. Mex., USA, 2002

[20] ***, Compendium of Neutron Spectra and Detector Responses for Radiation Protection Purposes – Supplement to Technical Report Series No. 318, Technical Report Series No. 403, International Atomic Energy Agency, Vienna, 2001

Received on July 17, 2009
Accepted on June 1, 2010

**Хашем МИРИ ХАКИМАБАД, Лале РАФАТ МОТАВАЛИ,
Кеихандокт КАРИМИ ШАХРИ**

УНИФОРМНОСТ ЈАЧИНЕ АКТИВАЦИЈЕ У БИЛАТЕРАЛНОМ IVNAA ПОСТРОЈЕЊУ ЗА ДВА АНТРОПОМОРФНА ФАНТОМА

Униформност активације је најважнији параметар у пројектовању уређаја за анализу гама зрака индукованих *ин-виво* неутронском активацијом. Прелиминарна анализа расподеле јачине активације у телу може се спровести коришћењем Монте Карло кодова као што је MCNP. У овом раду разматране су конфигурације система IVNAA са два неутронска извора, у циљу побољшања униформности јачине активације у воденом фантому димензија 32 cm 100 cm 16 cm. У најповољнијем случају, параметри униформности износе U = 1,003 и R = 1,67, уз средњу вредност јачине активације од 1,85 $^{-6}$ cm^{-3}. У циљу добијања тачнијих резултата, водени фантом је замењен моделом људског тела. Усвојени модел представља пет година стар ORNI-ов фантом испуњен меким ткивом. У овом случају унутрашњи органи нису симулирани. Коначне вредности параметара униформности за овај модел износе U = 1,005, и R = 12,2.

Кључне речи: униформност јачине активације, IVNAA са промптним гама зрацима, билатерална конфигурација, MCNP програм, фантом